Materials Research Proceedings 33 (2023) 41-48 https://doi.org/10.21741/9781644902677-7

DNS of momentum and heat transfer inside rough pipes

Mariangela De Maio[1,a *]

[1]Sapienza Università di Roma, Dipartimento di Ingegneria Meccanica e Aerospaziale, via Eudossiana 18, 00184 Roma, Italy

[a]mariangela.demaio@uniroma1.it

Keywords: Turbulent Flows, Pipe Flows, Roughness, DNS, Heat Transfer

Abstract. We carry out direct numerical simulation (DNS) of turbulent flow in pipes with a grit-blasted surface, to investigate both on momentum and heat transfer. A wide range of Reynolds numbers are considered, while maintaining a constant molecular Prandtl number of 0.7. The large relative roughness influences both the velocity and the temperature fields, indicating that the Reynolds analogy does not hold at high Reynolds bulk number.

Introduction

Pressure-driven flow in ducts is a subject of utmost relevance in mechanical and aerospace engineering applications.

Most simulations of forced convection in circular pipes have been carried out for the canonical case with smooth walls [1]. The case of rough walls is however at least as important, but so far it has mainly received attention through experimental studies and for surfaces with relatively low roughness. However, recent technological advances in the field of additive manufacturing have further prompted investigations of flow over surfaces with large relative roughness [2], which significantly affects both frictional drag and heat transfer. Understanding the behavior of flows over irregular rough surfaces with higher relative roughness than the ones studied in most experiments is thus certainly of great practical interest.

The systematic experimental investigation carried out by Nikuradse [3] is regarded as the starting point for the study of turbulent flows over rough walls. Nikuradse generated an extensive database for fully developed flow in circular pipes whose walls were covered with sieved sand grains. He identified three flow regimes: hydraulically smooth, transitionally rough, and fully-rough. In the first regime the height of the roughness is of the order of the viscous sublayer, hence roughness does not affect the flow. In the transitionally rough regime, the behavior of the flow instead depends strongly on the geometrical parameters of the roughness. Finally, in the fully-rough regime the friction coefficient is nearly unaffected by the Reynolds number. Generally, the friction factor increases with the relative roughness height, except for the laminar regime, where the friction factor of all the tested rough surfaces collapses to the smooth pipe case.

The presence of roughness affects both the mean flow and the turbulent motion of a fluid, which entails an increase of friction with respect to the smooth wall case. This is linked to the downward shift in the inner-scaled profile of the mean streamwise velocity, which can be expressed through the roughness function [4],

$$\Delta U^+ = U_S^+ - U_R^+, \quad (1)$$

where U_S^+ is the value of the mean streamwise velocity of the smooth case scaled in inner-units and U_R^+ is the one for the rough-wall case at the same friction Reynolds. The roughness function is computed in the logarithmic region of the velocity profiles, so that it can be unambiguously defined.

Materials Research Proceedings 33 (2023) 41-48 https://doi.org/10.21741/9781644902677-7

Nikuradse's investigation and more recent studies [5] [6] performed experiments with other types of rough surfaces and found that the velocity profiles of the rough-wall case collapse to the smooth-wall case if they are scaled in outer units. This result supports the validity of Townsend's outer-layer similarity hypothesis [7]. According to that hypothesis, smooth and rough wall turbulence behave similarly away from the wall at sufficiently high Reynolds number and at a sufficient scale separation between the typical roughness height (k) and the outer length scale of the flow (δ, e.g., the pipe diameter). Jiménez [8] stated that scale separation requires $k/\delta \lesssim 1/40$. However, several studies have shown that outer-layer similarity still holds in the wake region of the wall layer for surfaces with higher relative roughness [9] [10].

While the effect of wall roughness on momentum transfer is being extensively investigated, less attention has been given to the effect of wall roughness on turbulent heat transfer. Dipprey and Sabersky [11] performed some experiments over a granular surface and found that roughness augments momentum transfer more than heat transfer. The same result was found by Bons [12] who examined a number of realistic roughness geometries of gas turbine blades. On the other hand, so far direct numerical simulations (DNS) have been mainly focused on structured roughness [13]. Lately, more realistic surfaces have been investigated by Peeters et al. [10], who found an outer-layer similarity also for the temperature field. However, they also noticed a decrease in heat transfer efficiency at high Reynolds since momentum transfer is less increased than heat transfer with respect to the smooth-wall case.

The latter result is directly linked to the fact that the Reynolds Analogy hypothesis does not hold for a rough surface. According to this hypothesis the mean temperature field is similar to the velocity field. The discrepancy between the two fields can be quantified by the Reynolds Analogy Factor (RAF), which decreases as the efficiency in heat transfer diminishes.

Analogously to the velocity field, we can define a temperature roughness function,

$$\Delta\Theta^+ = \Theta_S^+ - \Theta_R^+ \tag{2}$$

In this case, the subtraction must be done both at the same friction Reynolds and at the same Prandtl number.

To sum up, the state of the art is mainly focused on relatively low roughness, and most of the DNS performed up to now consist of flows inside channels with infinite extensions in the spanwise direction. The present project aims at investigating the influence of relatively large roughness on the flow inside a circular pipe, with the goal of characterizing the differences between momentum and heat transfer. A relatively wide range of Reynolds numbers is investigated, up to the fully rough regime.

Numerical methodology

We use second-order finite-difference discretization of the incompressible Navier-Stokes equations in Cartesian coordinates, based on the classical marker-and-cell method [14] [15], with staggered arrangement of the flow variables to remove odd-even decoupling.

The divergence-free condition is enforced through the Poisson equation, which is solved by double trigonometric expansion in the streamwise and spanwise directions, and inversion of tridiagonal matrices in the third direction [16]. We use a hybrid third-order Runge-Kutta algorithm to perform the time integration. Furthermore, the convective terms are treated explicitly, whereas the diffusive terms are handled implicitly to alleviate the time step limitation. The mass flow rate is kept constant in time through a time-varying pressure gradient Π, which represents a uniform volumetric forcing applied to the streamwise momentum equation.

Similarly to the streamwise velocity field, the passive scalar equation is also forced with a time-varying, spatially homogeneous forcing term Q, in such a way that the integral of the temperature Θ over the pipe is strictly constant in time [17]. In the present simulations the constant passive

Materials Research Proceedings 33 (2023) 41-48 https://doi.org/10.21741/9781644902677-7

scalar value at the wall $\theta_w = 0$ is assigned as boundary condition and a Prandtl number $Pr = 0.7$ is assumed in all the simulations.

The computational domain is a rectangular box of size $L_x \times L_y \times L_z$, covered with a uniform Cartesian mesh of $N_x \times N_y \times N_z$ grid points. The rough pipe with mean radius R and cross-sectional area $A = \pi R^2$ is embedded in it. The no-slip boundary conditions and the temperature at the wall are approximately enforced through the immersed-boundary method.

As a preliminary step, the pipe geometry is generated in the standard Stereo-LiThography format, and a preprocessor based on the ray-tracing algorithm is used to discriminate grid points belonging to the fluid and to the solid [18]. Near the fluid-solid interface the viscous terms dominate the nonlinear and pressure terms, hence the boundary conditions can be enforced by locally changing the finite-difference weights for the approximation of the second derivatives [19].

The controlling parameter of the flow is the bulk Reynolds number $Re_b = 2Ru_b/\nu$, where u_b is the bulk velocity.

The resulting friction Reynolds number is $Re_\tau = Ru_\tau/\nu$, where the friction velocity is evaluated based on the measured pressure gradient, $u_\tau = \sqrt{\tau_w} = \sqrt{R/2 < \Pi >}$.

For normalization of the temperature field, we will consider the friction temperature, $\Theta_\tau = \frac{<q_w>}{u_\tau} = \frac{R}{2}\frac{<Q>}{u_\tau}$, where $< q_w >$ is the heat flux through the walls of the pipe.

The resistance that the fluid encounters inside the pipe is quantified through the friction coefficient, defined as

$$C_f = \frac{2\,\tau_w}{\rho\, u_b^2} \tag{3}$$

Whereas the overall heat transfer performance of the duct is quantified in terms of the Stanton number,

$$St = \frac{<q_w>}{\rho C_p u_b(\theta_w - \Theta_b)} \tag{4}$$

The bulk temperature can be computed as $\Theta_b = \frac{1}{A}\int_A U\theta dA$. In this case, the non-dimensional form for the previous equation is adopted, thus the density ρ and the specific heat C_p are equal 1.

Results

We consider a grit-blasted surface downloaded from the University of Southampton Institutional Repository [20]. The geometry has been scanned and post-processed, more information is reported in [21].

The pipe, shown in figure 1, is obtained by doubling the baseline samples in the spanwise direction and wrapping the obtained surfaces around the mean pipe geometry. In this study we define the roughness height to be the mean-peak-trough height (k), as obtained by partitioning the surface into 5 × 5 tiles of equal size, and then computing the average of the difference between the maximum and minimum height for each tile [22]. In the case of a rough surface another important parameter that needs to be defined is the roughness Reynolds number $k^+ = k\,u_\tau/\nu$.

Materials Research Proceedings 33 (2023) 41-48 https://doi.org/10.21741/9781644902677-7

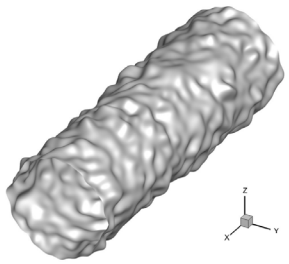

Figure 1 Pipe geometry obtained by wrapping the original rough surfaces around the pipe.

The results and the test conditions of the present DNS are listed in table 1. Since C_f is almost constant moving from $Re_b = 9800$ to 30000, we can state that the fully-rough regime is achieved.

Table 1 The definition of the first parameters is given in the text. $\Delta x^+, \Delta y^+$ *and* Δz^+ *are the grid spacings in the streamwise and cross-stream directions, given in wall units.* T *is the time interval used to collect the flow statistics, and* τ_t *is the eddy turnover time.*

Re_b	Re_τ	k^+	$C_f \times 10^2$	$St \times 10^3$	N_x	$N_y = N_z$	Δx^+	$\Delta z^+ = \Delta y^+$	T/τ_t	Symbol
500	32.75	6.08	3.43	17.09	384	192	0.53	0.42	104.77	
1000	46.69	8.70	1.75	8.58	384	192	0.76	0.60	74.70	
1500	58.41	10.89	1.21	5.83	384	192	0.96	0.75	62.29	
1750	64.78	12.03	1.10	5.16	384	192	1.06	0.83	59.40	
2500	123.73	23.07	1.95	9.21	384	192	2.01	1.58	79.05	
3000	149.88	27.94	2.00	9.26	384	192	2.45	1.92	79.94	●
4400	224.75	41.90	2.09	9.31	384	192	3.68	1.88	81.73	●
9800	521.67	97.25	2.27	9.01	960	480	3.41	2.67	85.17	●
30000	1613.49	300.02	2.30	8.14	1024	512	9.88	7.72	85.76	●

Figure 2 depicts the mean streamwise temperature distribution averaged over the cross section of the pipe, limited to the volume occupied by the fluid. The velocity isolines are superimposed on the temperature contours.

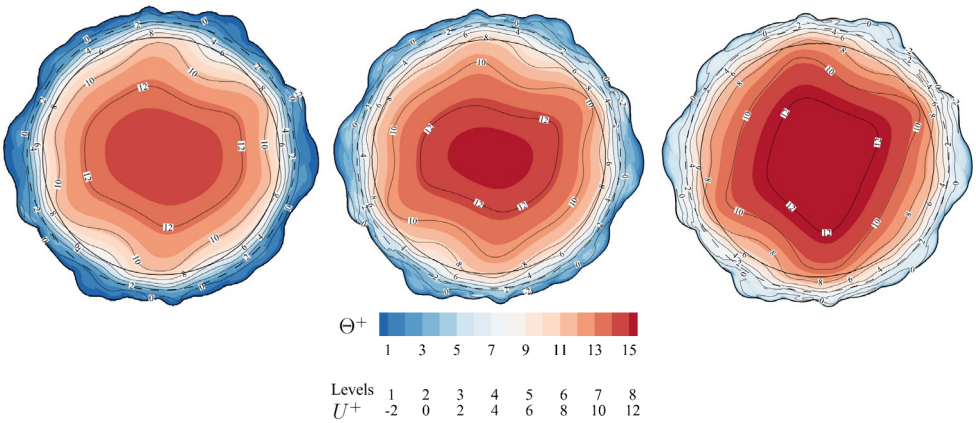

Figure 2 Contours of mean streamwise velocity for pipe at $\boldsymbol{Re_b = 4400}$ *(left),* $\boldsymbol{Re_b = 9800}$ *(centre) and* $\boldsymbol{Re_b = 30000}$ *(right). The black lines represent the velocity levels. The dashed circular line marks the position of the mean pipe surface, and the solid circular line marks the position of the plane of the crests.*

Owing to the large relative roughness, the fields do not show any symmetry, since the effect of the wall is felt throughout the wall layer. Furthermore, the fields iso-lines show clear sensitivity to Reynolds number variations and to the roughness geometry. As expected, temperature and velocity

Materials Research Proceedings 33 (2023) 41-48 https://doi.org/10.21741/9781644902677-7

contours present the same shape far from the wall, however they show some differences in the vicinity of the wall.

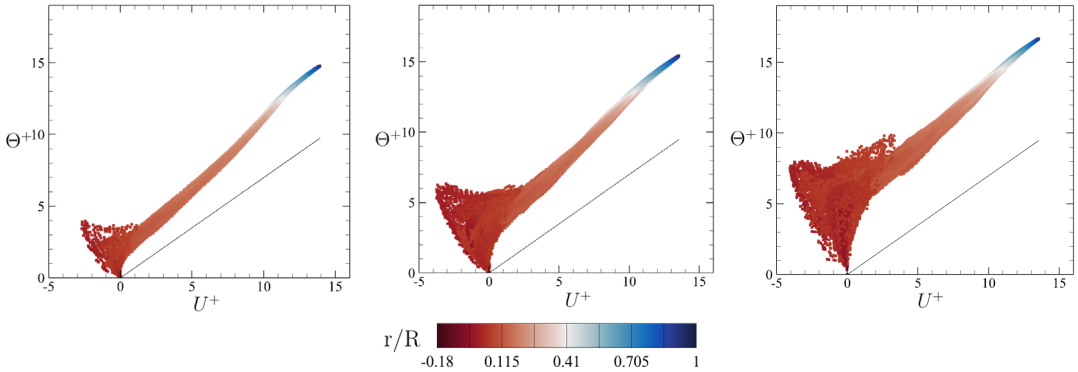

Figure 3 Scatter plot of mean temperature ($\boldsymbol{\Theta^+}$) versus mean velocity ($\boldsymbol{U^+}$) for pipe at $\boldsymbol{Re_b = 4400}$ (left), $\boldsymbol{Re_b = 9800}$ (centre) and $\boldsymbol{Re_b = 30000}$ (right). The black line corresponds to the ideal behaviour for the near-wall region in the smooth case, $\boldsymbol{\Theta^+ = Pr\, U^+}$.

These discrepancies are further investigated in figure 3, where we show a scatter plot of mean velocity and temperature scaled in inner units. The colors represent the distance from the mean radius R. In the smooth case a near equality of the two distributions occurs and a linear relationship between the velocity and temperature fields is expected near the wall, $\Theta^+ = Pr\ U^+$. The same does not happen for the rough wall case, where a large scatter between Θ^+ and U^+ occurs near the walls. This is owed to the presence of the recirculation zones where the velocity reaches negative values, whereas the temperature present always positive values. Moreover, the scatter increases with Reynolds bulk since the strength of the recirculation zone increases and the velocity reaches lower mean velocity values. Furthermore, hotter fluid can flow from the bulk region towards the wall, which leads to higher mean temperatures inside the roughness layer [10]. Far from the wall the scatter decreases, also reflecting the similarity of the shapes of the contours in figure 2. However, the temperature presents much higher values than the mean streamwise velocity.

Figure 4 shows the defect velocity profiles of the mean streamwise velocity and temperature. Some scatter is observed near the walls, but both the temperature and the velocity profiles tend to collapse far from it. Despite large relative roughness, our DNS provides evidence that the outer layer similarity is achieved even if $k/R \approx 1/5$.

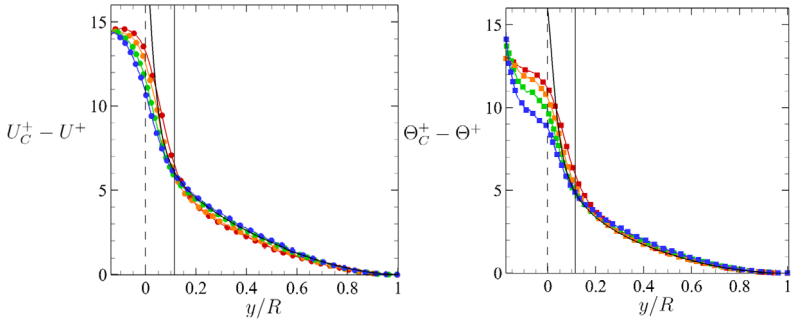

Figure 4 Velocity (left) defect profiles and temperature (right) defect profiles at various $\boldsymbol{Re_b}$, with colors defined in table 1. The black line corresponds to the smooth wall case. The vertical solid line corresponds to the plane of the crests and the dashed like marks the mean pipe surface $y/R = 0$.

The validity of the outer-layer similarity permits to identify a logarithmic region, even if with narrow extent. This is necessary to properly define both velocity and temperature roughness functions.

Materials Research Proceedings 33 (2023) 41-48 https://doi.org/10.21741/9781644902677-7

Figure 5 shows the roughness functions for our DNS as function of k^+, the data from Nikuradse's experiment [3] and the fully-rough asymptote. Velocity roughness function (red circles) has a trend quite similar to that observed in Nikuradse's experiments (black circles). It can be noticed that the velocity roughness function is always increasing with k^+, whereas the temperature roughness function (red squares) has a gradual increase, and it is believed to reach a plateau for high roughness Reynolds numbers [10]. This is directly correlated to the fact that at high Reynolds number the increase in friction with respect to the smooth case is higher than heat transfer augmentation.

As customary we proceed to determine values of the equivalent sand-grain roughness height, by enforcing universality of the roughness function to the fully-rough asymptote of Nikuradse. Data fitting of our DNS results yields $k_s^+ = 0.76\,k^+$ for the surface under consideration. For completeness, we recall that there is no universal behavior in the fully rough regime for the temperature roughness function since the results of previous studies present a wide scatter.

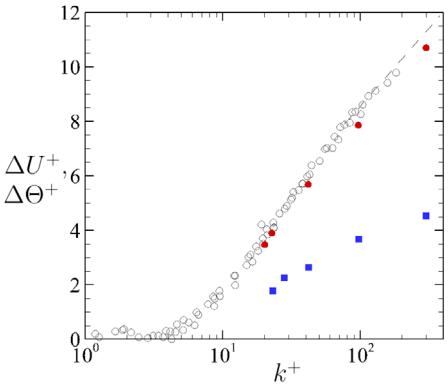

Figure 5 Variation of the velocity roughness function (red circles) and the temperature roughness function (blue squares) with inner-scale roughness height. Empty circles represent Nikuradse's results and the dashed line is the fully-rough asymptote.

Left panel of figure 6 shows the friction coefficient and the Stanton number obtained from the present DNS as functions of the Reynolds numbers. Referring to the laminar flow region in the low-Re end of the graph, in Nikuradse's experiments the friction factor for all surfaces collapsed to the Hagen-Poiseuille prediction $f = 4C_f = 64/Re_b$, thus suggesting that friction is not affected by the change of the wall geometry. In the present DNS we notice that the computed friction factors are higher than the expected theoretical values by about 7% for the present simulations. This indicates that in our case the larger relative roughness has the role of altering the geometry of the pipe, thus producing modification also in the laminar flow regime. The same result was found by Huang et al. [23], who noticed that as the relative roughness becomes larger, the friction coefficient increases also in the laminar region.

After the transition from laminar to turbulent flow, both the friction factor and the Stanton number start increasing. At the highest Reynolds numbers, C_f attains almost to a constant value, and the fully-rough regime is reached. Since the Stanton number is the thermal counterpart of the friction coefficient, one would expect a constant value of the Stanton number in the fully-rough regime. However, the plot shows that it decreases at the highest Reynolds numbers. Furthermore, in the transitional rough regime the Stanton number is almost constant, as if the fully-rough regime is reached at lower Reynolds number for the temperature field. Similar results have been found by Forooghi et al. [24], who addressed this behavior to the thinner boundary layer of the temperature with respect to the velocity at Prandtl 0.7.

Right panel of figure 6 shows the trend of the ratio between the Reynolds Analogy Factor of the rough (RAF) and smooth case ($\boldsymbol{RAF_S}$) as a function of Reynolds bulk for the flow in the

turbulent regime. In accordance with previous studies [9] [12], the Reynolds Analogy Factor decreases with respect to the smooth pipe, this is due to the fact that roughness augments momentum transfer more than heat transfer. As the Reynolds number increases, the efficiency in heat transfer decreases and so does RAF.

Indeed, at low Re_b the viscous transport is still important, and hence, the value of RAF is closer to that of a smooth wall. Whereas, in the fully-rough regime the resistance of the flow is mainly due to the pressure or form drag and not to the viscous drag. However, there is no enhancement mechanism for heat transfer comparable to the pressure, this explains why heat transfer is not increased by roughness as much as skin friction, especially for high Reynolds numbers.

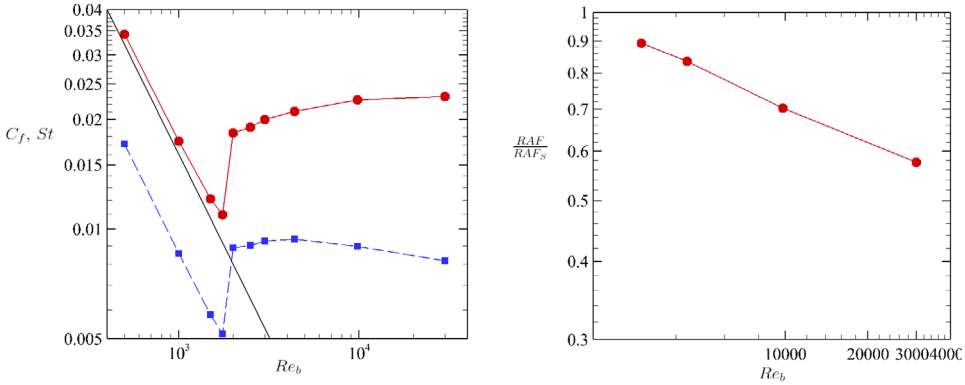

Figure 6 Right: Variation of St (blue squares) and $\boldsymbol{C_f}$ *(red circles) with the Reynolds bulk. The black lines represent Hagen-Poiseuille prediction* $\boldsymbol{C_f = 16/Re_b}$.
Left: Variation of the $\boldsymbol{RAF/RAF_S}$ *coefficient with the Reynolds bulk, for* $\boldsymbol{Re_b \geq 3000}$.

Summary

To conclude, it is evident that the presence of rough walls influences both the velocity and the temperature fields. Moreover, the large relative roughness influences the flow also in the laminar region, as if the roughness modified the shape of the cross-section of the pipe. Last, it is evident that the Reynolds analogy does not hold, as the Reynolds bulk increases. The latter result is a very important since the industrial design of the cooling channels is based on the use of the Reynolds-averaged Navier-Stokes equations (RANS), which could rely on the Reynolds analogy, thus yielding an overprediction of the heat transfer.

Follow-up studies should include DNS of flows over new rough surfaces. The resulting database could then be used to develop improved predictive correlations for heat transfer and for the tuning of the RANS simulations.

References

[1] S. Pirozzoli, J. Romero, M. Fatica, R. Verzicco e P. Orlandi, «DNS of passive scalars in turbulent pipe flow,» *J. Fluid Mech.,* 940, A45, 2022. https://doi.org/10.1017/jfm.2022.265

[2] C. Stimpson, J. Snyder, K. Thole e D. Mongillo, «Roughness effects on flow and heat transfer for additively manufactured channels.,» *J. Turbomach.,* 138(5):051008, 2016. https://doi.org/10.1115/1.4032167

[3] J. Nikuradse, Strömungsgesetze in rauhen rohren, 1933.

[4] F. Hama, « Boundary layer characteristics for smooth and rough surfaces,» *Trans. Soc. Nav. Arch. Marine Engrs.,* 62:333–358, 1954.

[5] M. Shockling, J. Allen e A. Smits, «Roughness effects in turbulent pipe flow,» *J. Fluid Mech.,* 564:267–285, 2006. https://doi.org/10.1017/S0022112006001467

[6] M. Flack e K. Schultz, «The rough-wall turbulent boundary layer from the hydraulically smooth to the fully rough regime», *J. Fluid Mech.,* 580:381–405, 2007. https://doi.org/10.1017/S0022112007005502

[7] A. Townsend, «The structure of turbulent shear flow», *Cambridge University press,* 1976.

[8] J. Jimenez, «Turbulent flows over rough walls», *Annu. Rev. Fluid Mech.,* 36:173–196, 2004. https://doi/10.1146/annurev.fluid.36.050802.122103

[9] P. Forooghi, M. Stripf e B. Frohnapfel, «A systematic study of turbulent heat transfer over rough walls», *Int. J. Heat Mass Transf.,* 127, 1157-1168, 2018. https://doi.org/10.1016/j.ijheatmasstransfer.2018.08.013

[10] J. W. R. Peeters e N. D. Sandham, «Turbulent heat transfer in channels with irregular roughness», *Int. J. Heatm Mass Transf.,* 138:454-467, 2019. https://doi.org/10.1016/j.ijheatmasstransfer.2019.04.013

[11] D. Dipprey e R. Sabersky, «Heat and momentum transfer in smooth and rough tubes at various Prandtl numbers», *Int. J. Heat Mass Transf.,* 6:329-353, 1963. https://doi.org/10.1016/0017-9310(63)90097-8

[12] J. Bons, «A Critical Assessment of Reynolds Analogy for Turbine Flows», *J. Heat Transf.,* 127(5): 472–485, 2005. https://doi.org/10.1115/1.1861919

[13] P. Orlandi, D. Sassun e S. Leonardi, «DNS of conjugate heat transfer in presence of rough surfaces», *Int. J. Heat Mass Transf.,* 100: 250-266., 2016. https://doi.org/10.1016/j.ijheatmasstransfer.2016.04.035

[14] J. Welch e F. Harlow, «Numerical calculation of time-dependent viscous incompressible flow of fluid with free surface», *Phys. Fluids,* 8(12):2182, 1956. https://doi.org/10.1063/1.1761178

[15] P. Orlandi, «Fluid flow phenomena: a numerical toolkit», in *Springer Science & Business Media*, 2000, 55.

[16] P. Moin e J. Kim, «Application of a fractional-step method to incompressible Navier-Stokes equations», *J. Comput. Phys.,* 59:308–323, 1985. https://doi.org/10.1016/0021-9991(85)90148-2

[17] S. Pirozzoli, M. Bernardini e P. Orlandi, «Passive scalars in turbulent channel flow at high Reynolds number», *J. Fluid Mech.,* 788, 614-639., 2016. https://doi.org/10.1017/jfm.2015.711

[18] G. Iaccarino e R. Verzicco, «Immersed boundary technique for turbulent flow simulations», *Appl. Mech. Rev.,* 56(3):331–347, 2003. https://doi.org/10.1115/1.1563627

[19] S. Leonardi e P. Orlandi, «DNS of turbulent channel flows with two-and three-dimensional roughness», *J. Turbul.,* 7:N73, 2006. https://doi.org/10.1080/14685240600827526

[20] M. Thakkar, A. Busse e N. D. Sandham, «Dataset for surface correlations of hydrodynamic drag for transitionally rough engineering surfaces», 2016. [Online]. Available: https://eprints.soton.ac.uk/392562/.

[21] A. Busse, M. Lützner e N. Sandham, «Direct numerical simulation of turbulent flow over a rough surface based on a surface scan», *Comp. Fluids,* 116, 129-147, 2015. https://doi.org/10.1016/j.compfluid.2015.04.008

[22] M. Thakkar, A. Busse e N. D. Sandham, «Surface correlations of hydrodynamic drag for transitionally rough», *J. Turbul.,* 8(2):138–169, 2017. https://doi.org/10.1080/14685248.2016.1258119

[23] K. Huang, J. Wan, C. Chen, Y. Li, D. Mao e Z. M.Y., «Experimental investigation on friction factor in pipes with large roughness», *Exp. Therm. Fluid Sci.,* 50:147–153, 2013. https://doi.org/10.1016/j.expthermflusci.2013.06.002

[24] P. Forooghi, A. Weidenlener, F. Magagnato, B. Böhm, H. Kubach, T. Koch e B. Frohnapfel, «DNS of momentum and heat transfer over rough surfaces based on realistic combustion chamber deposit geometries», *Int. J. Heat Fluid,* 2018. https://doi.org/10.1016/j.ijheatfluidflow.2017.12.002